

Synthesis of Near-Infrared Bandgap Lead Sulfide Quantum Dots to Mimic the Solar Spectrum

Uday Das

Department of Physics, Hooghly Mohsin College, Chinsurah, Hooghly-712101, West Bengal, India

Email: udaydas_ju[at]yahoo.co.in

Published on: 20.05.2023

Abstract: *The limiting efficiency for a conventional single junction solar cell is restricted to 32%, known as Shockley–Queisser limit. Commercially successful monocrystalline silicon (c-Si) solar cells reached 26.8%, and emerging perovskite solar cells achieved 25.2% efficiency on a lab scale. Most of the contemporary solar cell technologies and research are focused on replacing silicon with inexpensive materials and processes to reduce the KW/hr cost of solar cells. However, materials used for the development of single-junction solar cells (c-Si, perovskite, organic dyes, and polymers) only harness a part of the solar spectrum, leaving behind a significant unused NIR spectrum (~50% of the solar energy). Utilization of the unused NIR solar radiation in tandem solar cell architecture would lead to significantly higher efficiency (~45% for two junction tandem solar cells). However, the scarcity of desired low bandgap materials is the Achilles' heel for the utilization of NIR photons in solar cells. Though a few III-V class compound semiconductors have the desired NIR band gaps, material scarcity and the requirement of sophisticated processing techniques hinder their large-scale utilization. Herein I showcase the synthesis of NIR bandgap lead sulfide (PbS) quantum dots (QDs) mimicking the solar spectrum. The as-synthesized QDs show an absorption onset of 1350 nm (0.92 eV), which is ideal for the two-junction tandem solar cell development. Optical characterizations of as-synthesized QDs are performed via absorption and emission spectroscopy, and the structural characterizations are carried out by X-ray diffraction (XRD) and transmission electron microscopy (TEM).*

Keywords: NIR Bandgap, PbS quantum dots, NIR optoelectronic devices

1. Introduction

Commercially successful monocrystalline Silicon (c-Si) and the emerging perovskite-based single-junction solar cells have reached power conversion efficiency (PCE) of 26.1% and 25.2%, respectively, in the laboratory environment [1]. Despite high PCE values, c-Si transmits 20% and perovskite 43% of the incident NIR solar radiation, providing a huge opportunity to boost their efficiency through better spectral utilization [2, 3]. Some III-V class semiconductors absorb these NIR solar radiations to yield high efficiencies in multi-junction solar cells, but high material costs, expensive processing techniques, and complex concentrator requirement have limited their large-scale commercial prospects [4]. Low-cost alternatives like organic polymers and dyes are also ineffective in harnessing the NIR range photons [5, 6]. Tunable bandgap solution-processed QDs can be a potential solution to this problem. Their bandgap can be precisely tuned in the NIR range to match the requirement via facile size control [7].

Broad tunability of the energy bandgap through size control makes the colloidal quantum dots (QDs) promising for the development of photovoltaic devices. NIR bandgap QDs are particularly interesting as they can be used to augment perovskite and c-Si solar cells due to their complementary NIR absorption. Lead sulfide (PbS) QDs have spurred intense interest in photovoltaic applications due to their wide spectral tunability, direct bandgap, ambient stability, and solution phase processability [8-11]. However, most of the research efforts are concentrated on developing solar cells based on 1.3eV bandgap PbS QDs, as the bandgap is ideal for the single-junction solar cells. There are few studies on the development of narrow bandgap QDs (< 1eV), suitable for tandem solar cell applications. Using detailed charge balance calculation, it is shown that NIR QDs can produce additional efficiency points up to 12% and 5% when used in

tandem with perovskite and c-Si solar cells, respectively [3, 4].

Herein, a chemical root synthetic strategy is developed to produce high-quality PbS QDs targeting their application in tandem solar cell devices. The synthesis parameters are devised to yield 0.92 eV bandgap QDs which is most suitable to mimic the solar spectrum and ideal for the two-junction tandem solar cell applications. Optical characterizations of as-synthesized QDs show strong excitonic absorption and band-edge emission. Structural characterizations show crystalline PbS QDs with a high degree of monodispersity.

2. Experimental Section

Oleic acid (OA; 90%), lead oxide (PbO; 99%), bis-(trimethylsilyl) sulfide (TMS), 1-octadecene (ODE; 90%), lead bromide (PbBr₂; 99%) and Oleylamine (70%), chloroform, toluene and acetone are purchased from Sigma-Aldrich and used as received.

Synthesis of 0.92 eV PbS QDs: PbS QDs with an absorption onset of 0.92 eV were synthesized using the following approach. In a three-necked round-bottomed flask, 1.8 g of PbO, 12 ml of ODE, and 6 ml of OA were combined before being degassed at 110 °C for 12 h while being constantly stirred. The reaction temperature was set to 100°C, and 15ml of ODE was added to the reaction mixture and kept under vacuum for 30 min. The reaction medium was switched from vacuum to argon, and the temperature was increased to 125 °C, in preparation for the injection of the sulphur precursor. Using a syringe, 240 µl of TMS dissolved in 9 ml of ODE was rapidly injected into the reaction mixture, and the temperature source was switched off. 1ml of 1mM PbBr₂ in Oleylamine was added once the reaction medium had reached 60°C. 10 ml of acetone was added to the reaction mixture at 30°C and stirred for an additional 5 minutes.

Volume 12 Issue 5, May 2023

www.ijsr.net

Licensed Under Creative Commons Attribution CC BY

After that, the synthesized material was divided among numerous test tubes, and more acetone was added in order to separate the QDs from the solution. To isolate the QDs, the test tubes were centrifuged at 3000 RPM, and the supernatant was removed. Toluene was used to disperse the QDs, and then acetone was used to precipitate them once more. After being separated by centrifugation, the QDs were dried for five minutes in a vacuum. The QDs were then dispersed in chloroform and kept for future characterizations.

-PbBr₂ precursor preparation: PbBr₂ was dissolved in Oleylamine at the concentration of 1mM/ml and kept under vacuum for 1hr at 100°C prior to their use.

Material characterization: Shimadzu UV-VIS-IR (UV-3600 Plus) spectrometer and an integrating sphere (ISR-603) are used for absorbance measurements. Emission spectrums are recorded using a spectrofluorometer (FS5, Edinburg Instrument). XRD profiles are recorded on an X'pert Pro model PANalytical diffractometer from Philips PANalytical instruments operated at a voltage of 40 kV and a current of 30 mA with Cu K α (1.5418 Å) radiation. The QDs and ligand samples are scanned for the 2 θ range of 10° to 80° with a scan rate of 0.4° per minute. TEM imaging is done using a high-resolution transmission electron microscope (JEOL JEM 2200FES).

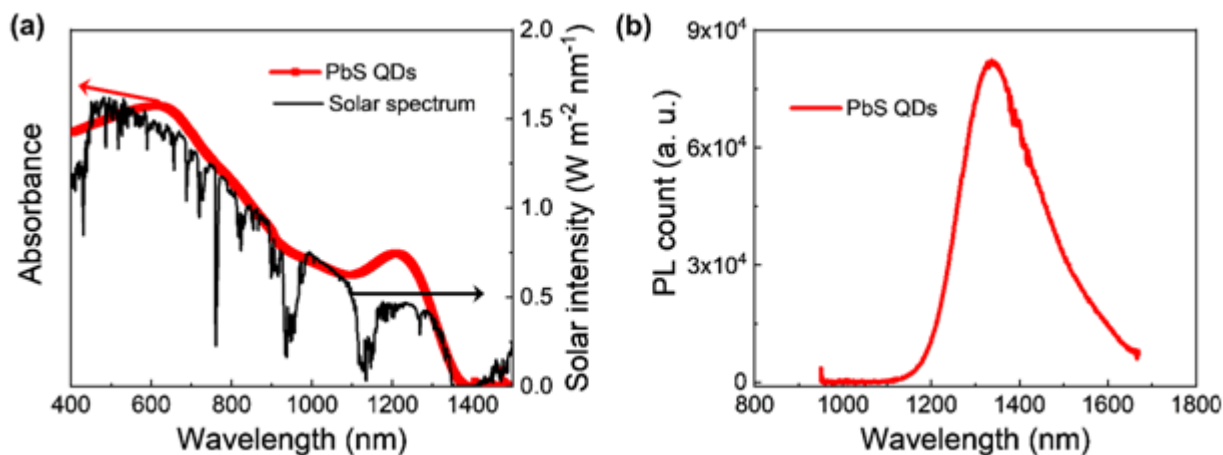


Figure 1: (a) Absorbance spectrum of PbS QD film on a quartz substrate. The AM 1.5G solar spectrum is shown along the right-hand axis. The absorbance spectrum of PbS QDs mimics the solar spectrum with an absorption onset of 1352 nm (0.92 eV). (b) The emission spectrum of PbS QD films shows strong band edge emission with a Stokes shift of 90 meV.

3. Results & Discussion

For optical characterization as synthesized oleic acid-capped PbS QDs are deposited on quartz substrates using the doctor's blending technique. The absorption spectrum of PbS QD film on a quartz substrate is shown in Figure 1a. The absorption onset for the PbS QD films is found to be 1365 nm, and the first excitonic peak appears at 1211 nm. The energy bandgap corresponding to the first excitonic peak is 1.02 eV. The absorption spectrum of PbS QDs mimics the solar spectrum, as shown along the right-hand side axis of

Figure 1a. The near-perfect matching of the PbS QD's absorption spectrum with the solar spectrum is highly desirable for solar cell applications. The emission properties of the PbS QD film show strong band-edge emission, with the emission peak at 1337 nm. The Stokes' shift calculated from the energy difference between the first excitonic peak and the emission peak is found to be 96 meV. Intense band-edge emission and a relatively low Stokes' shift indicate a high degree of size uniformity and well-passivated surface states in synthesized PbS QDs.

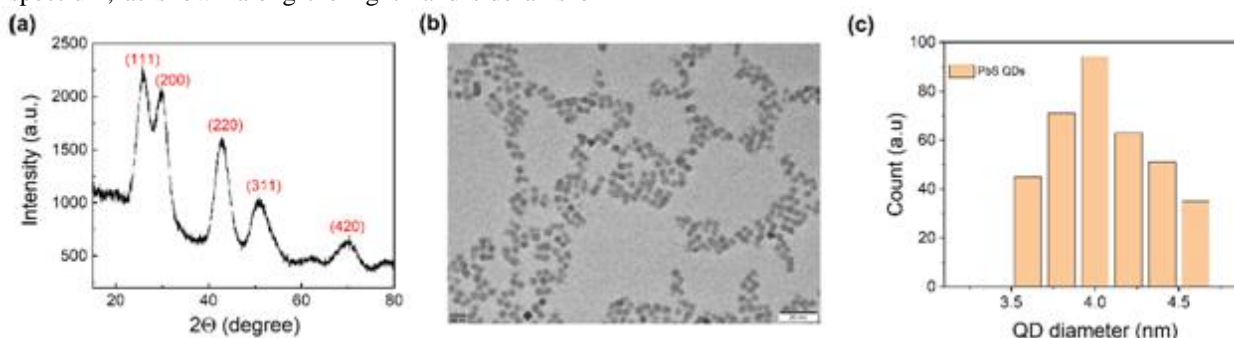


Figure 2: (a) XRD spectrum of PbS QD film. The characteristic peaks indicate the rock salt structure of PbS. (b) The high-resolution TEM image indicating monodisperse PbS QDs. (c) Shows the size distribution of QDs determined from the TEM image

The structural characterization of the PbS QDs is carried out by X-ray diffraction (XRD) measurement. The XRD plot (Figure 2a) shows well-defined diffraction peaks for planes

(111), (200), (220), (311), and (420) for the corresponding 2 θ values at 25.88, 29.68, 42.83, 50.83, 69.84 degrees, respectively. The XRD spectrum matches with the reference

XRD file of PbS: JCPDS-78-1901. XRD spectrum confirms the face-centered cubic crystal structure of PbS QDs. The broadening of the diffraction peak indicated nano-dimensioned crystals of PbS QDs. To determine the size of PbS QDs, transmission electron microscopy (TEM) imaging was carried out. The diluted solution of PbS QDs was drop-cast on TEM grid and allowed to dry in ambient conditions for sample preparation. TEM image shows a uniform distribution of PbS QDs on the TEM grid (Figure 2b). The size distribution of PbS QDs determined from the TEM image shows an average particle diameter of 4 ± 0.5 nm (Figure 2c).

4. Conclusion

In summary, NIR bandgap PbS QDs are successfully synthesized to mimic the broad-range solar spectrum. Optical and structural characterizations confirm a high degree of size uniformity and good absorption and emission properties of as-synthesized PbS QDs. The developed synthetic strategy for NIR band gap PbS QDs would be widely useful in solar cells and other NIR optoelectronic devices.

References

- [1] B. R.-C. National Renewable Energy Laboratory and E. C. <https://www.nrel.gov/pv/assets/pdfs/best-research-cell-efficiencies.20200218.pdf>.
- [2] A. H. Ip, A. Kiani, I. J. Kramer, O. Voznyy, H. F. Movahed, L. Levina, M. M. Adachi, S. Hoogland, E. H. Sargent; *Acs Nano*, **2015**, 9 (9), 8833-8842.
- [3] E. H. Sargent; *Nat. Photonics*, **2009**, 3 (6), 325-331.
- [4] H. Cotal, C. Fetzer, J. Boisvert, G. Kinsey, R. King, P. Hebert, H. Yoon, N. Karam; *Energy Environ. Sci.* **2009**, 2 (2), 174-192.
- [5] W. W. Li, K. H. Hendriks, W. S. C. Roelofs, Y. Kim, M. M. Wienk, R. A. J. Janssen; *Adv. Mater.* **2013**, 25 (23), 3182-3186.
- [6] S. Mathew, A. Yella, P. Gao, R. Humphry-Baker, B. F. E. Curchod, N. Ashari-Astani, I. Tavernelli, U. Rothlisberger, M. K. Nazeeruddin, M. Gratzel; *Nat. Chem.* **2014**, 6 (3), 242-247.
- [7] M. A. Hines, G. D. Scholes; *Adv. Mater.* **2003**, 15 (21), 1844-1849.
- [8] I. J. Kramer, E. H. Sargent; *Acs Nano* **2011**, 5 (11), 8506-8514.
- [9] C. H. M. Chuang, P. R. Brown, V. Bulovic, M. G. Bawendi; *Nat. Mater.* **2014**, 13 (8), 796-801.
- [10] O. Ouellette, N. Hossain, B. R. Sutherland, A. Kiani, F. P. G. de Arquer, H. R. Tan, M. Chaker, S. Hoogland, E. H. Sargent; *Acs Energy Lett.* **2016**, 1 (4), 852-857.
- [11] B. Sun, A. Johnston, C. Xu, M. Y. Wei, Z. R. Huang, Z. Jiang, H. Zhou, Y. J. Gao, Y. T. Dong, O. Ouellette, X. P. Zheng, J. K. Liu, M. J. Choi, Y. Gao, S. W. Baek, F. Laquai, O. M. Bakr, D. Y. Ban, O. Voznyy, F. P. G. de Arquer, E. H. Sargent; *Joule* **2020**, 4 (7), 1542-1556.